ON THE COVERAGE OF A RANDOM SENSOR NETWORK IN A BOUNDED DOMAIN

Henri Koskinen
Networking Laboratory, Helsinki University of Technology,
P.O. Box 3000, FIN 02015 HUT, Finland
e-mail: Henri.Koskinen@hut.fi
Phone: +358 9 451 5429. Fax: +358 9 451 2474.

ABSTRACT

We examine the area coverage of random sensor networks in bounded domains under a Boolean coverage disk model where all sensors are assumed to have a common sensing range. We solve the expected area coverage analytically for a circular domain with border effects and for an arbitrary bounded domain without border effects, i.e., when the locations of the sensors are and are not, respectively, confined to the domain to be covered. We also consider the problem of full coverage of the domain and recognize that this problem, like that of network connectivity, reduces to the problem of determining the distribution of a well-defined threshold range. Focusing on a square domain, again with and without border effects, we utilize existing asymptotic results in building empirical regression models for the threshold range for full coverage. These models allow predicting the relation between the parameters of the sensor network and the probability of full coverage.

1 Introduction

In [1], Liu and Towsley defined different coverage and detectability quantities of wireless sensor networks. For instance, modelling the sensing area of a single sensor as a disk characterized by a common sensing range, they defined the *area coverage* f_a as the fraction of the geographical area that is within this sensing range from at least one sensor. In the case of random sensor networks, they determined the area coverage in the infinite plane using known results of homogeneous Poisson point processes.

The analysis of random sensor networks is motivated by visions where large amounts of tiny sensors, often referred to as "smart dust", are scattered over some terrain from, say, an aircraft. Sensor mobility is another element that can incorporate randomness into sensor locations.

However, the finiteness of realistic scenarios is something that should be taken into account in the analysis. This is the goal of this paper. We address the area coverage f_a of a random sensor network in a bounded domain. In this case, the area coverage is a random variable with a continuous probability distribution between 0% and 100% and point probabilities at 0% and 100%. We solve $\mathrm{E}f_a$ analytically for a circular domain with border effects and for an arbitrary bounded domain without border effects, i.e., when the locations of the sensors are and are not, respectively, confined to the domain to be covered.

We also consider the problem of full coverage characterized by $\mathrm{P}(f_a = 100\%)$, which constitutes the major part of this paper. This problem resembles that of connectivity of a multihop network under a similar Boolean model: if all network nodes are assumed to have a common transmission range within which direct communication is possible, the connectivity of random networks boils down to the distribution of the greatest edge length in the minimum spanning tree of the nodes, which is the threshold range for connectivity as pointed out in [2]. This distribution is known only asymptotically and is given in [3]. In this paper, we show that the problem of full coverage also reduces to determining the distribution of a threshold range which is now found from the Voronoi diagram of the nodes. We recognize that the analytical results derived by Janson in [4] can be interpreted as the asymptotic distribution of the threshold range for full coverage when border effects are eliminated. We present an approximate extension of this distribution to the case involving border effects. Focusing on a square domain, with and without border effects, these distributions are taken as the bases for empirical regression models that can be used to predict full coverage.

This paper is structured as follows. The next section concentrates on expected area coverage, first focusing on a case involving border effects and then on one free of border effects. The problem of full coverage is considered in Section 3. Starting with the related analytical results, the section then presents the empirical models along with their diagnostics and validation. Section 4 concludes the paper.

2 Expected area coverage

Suppose that a given number of sensors with a common sensing range r are randomly and uniformly distributed

over a bounded domain. We wish to determine the expected area coverage in the domain, which is equivalent to determining the probability that a random point inside the domain is covered. This probability, in turn, depends on whether or not sensors are also distributed outside the domain: if not, points at the boundary of the domain are less likely to be covered than those in the interior. This is referred to as the border effect.

2.1 A setting with border effect

Assume now that the domain is a circular disk with radius R and center at the origin O and that n sensors are randomly placed on the disk. Given a point x on the disk, the probability that it is *not* covered by any of the sensors is $(1-|\mathcal{B}_x(r) \bigcap \mathcal{B}_O(R)|/(\pi R^2))^n$, where $\mathcal{B}_x(r)$ denotes the disk with radius r centered at x and $|\mathcal{B}_x(r)|$ its area. The area of the intersection depends on the radial coordinate ρ of x: if $\rho \leq |R-r|$, (allowing also $r > R$,) it is equal to $\min\{\pi r^2, \pi R^2\}$. If $\rho > |R-r|$, it is given by

$$A(\rho,R,r) = \frac{-\sqrt{(-\rho+r+R)(\rho+r-R)(\rho-r+R)(\rho+r+R)}}{2} + r^2 \arccos\left(\frac{\rho^2+r^2-R^2}{2\,\rho\,r}\right) + R^2 \arccos\left(\frac{\rho^2-r^2+R^2}{2\,\rho\,R}\right)$$

as presented in [5]. The overall probability is obtained by conditioning on ρ:
P(not covered) $= \int_\rho$ P(not covered$|\rho) f(\rho) d\rho$, where $f(\rho)$ is the probability density function of ρ. For uniform density all over the disk, we have $f(\rho) = \frac{d}{d\rho}((\pi\rho^2)/(\pi R^2)) = 2\rho/R^2$. We finally get the expected area coverage:

$$\begin{aligned} \mathrm{E}f_a &= 1-\text{P(not covered)} \\ &= 1-\left[\frac{\pi(R-r)^2}{\pi R^2}\left(1-\frac{\min\{\pi r^2,\pi R^2\}}{\pi R^2}\right)^n + \int_{|R-r|}^{R} \frac{2\rho}{R^2}\left(1-\frac{A(\rho,R,r)}{\pi R^2}\right)^n d\rho\right]. \end{aligned} \quad (1)$$

2.2 A setting without border effect

Now let the domain to be covered be a bounded set $\mathcal{D}$ in the plane and assume that the n sensors are uniformly distributed on a larger set that contains all points within the range r from $\mathcal{D}$ (hence there is no border effect). Let the area of this larger set be A. Then we simply have P(not covered) $= (1-\pi r^2/A)^n$ for all points inside $\mathcal{D}$. Denoting the average node density by $\lambda = n/A$ and substituting $n = \lambda A$ yields for fixed λ and r

$$\begin{aligned} \lim_{A\to\infty} \mathrm{E}f_a &= 1 - \lim_{A\to\infty} \text{P(not covered)} \\ &= 1-\exp(-\lambda\pi r^2), \end{aligned} \quad (2)$$

which is equal to the area coverage in the infinite plane given in [1]. Note however that while this is the exact area coverage in the infinite plane, it is only the expected area coverage in $\mathcal{D}$, and with $\lambda, r > 0$, the distribution of f_a is nonzero in the whole interval including 0% and 100%.

Note also that we get the same limit from (1) for fixed r and $\lambda = n/(\pi R^2)$ by substituting $n = \lambda\pi R^2$ and letting $R \to \infty$, because the weight of the integral term – the border zone – diminishes. Letting the circular disk grow infinitely therefore gives the result of the infinite plane. In this limit, however, the distribution of f_a narrows down to a single known value.

Figure 1 illustrates how the border effect affects the expected area coverage.

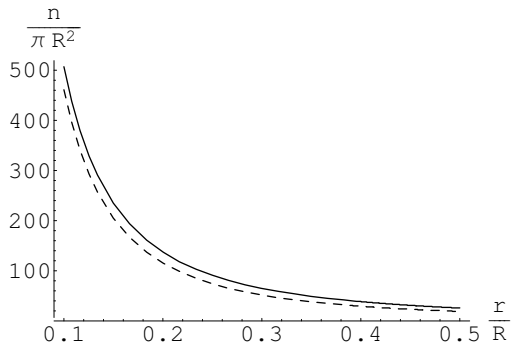

Figure 1: The number of nodes (per area πR^2) required to ensure $\mathrm{E}f_a = 99\%$ on a disk with radius R when r/R ranges from 0.1 to 0.5, in a setting with border effect (using (1) numerically; solid line) and without border effect (using (2) with $\lambda = n/(\pi R^2)$; dashed line).

3 Probability of full coverage

3.1 Analytical treatment

In the problem of full coverage, we are interested in characterizing P($f_a = 100\%$) as a function of the sensor density and the sensing range when the sensors are assumed to be placed uniformly at random over some target domain. This problem is equivalent to finding the distribution of the *threshold range* for full coverage (conditional to the sensor density): for a given set of sensors with known locations, we define the threshold range for full coverage as the smallest value of the sensing range for which the target domain is completely covered by the sensors. The probability that a random set of sensors with sensing range r completely covers the domain then equals the cumulative distribution function of this threshold range, evaluated at r.

Like the expected area coverage, the probability of full coverage largely depends on whether or not the locations of the sensors are confined to the bounded target domain. Figure 2 shows an example of both cases: for a set of sensors located inside the domain, the threshold range

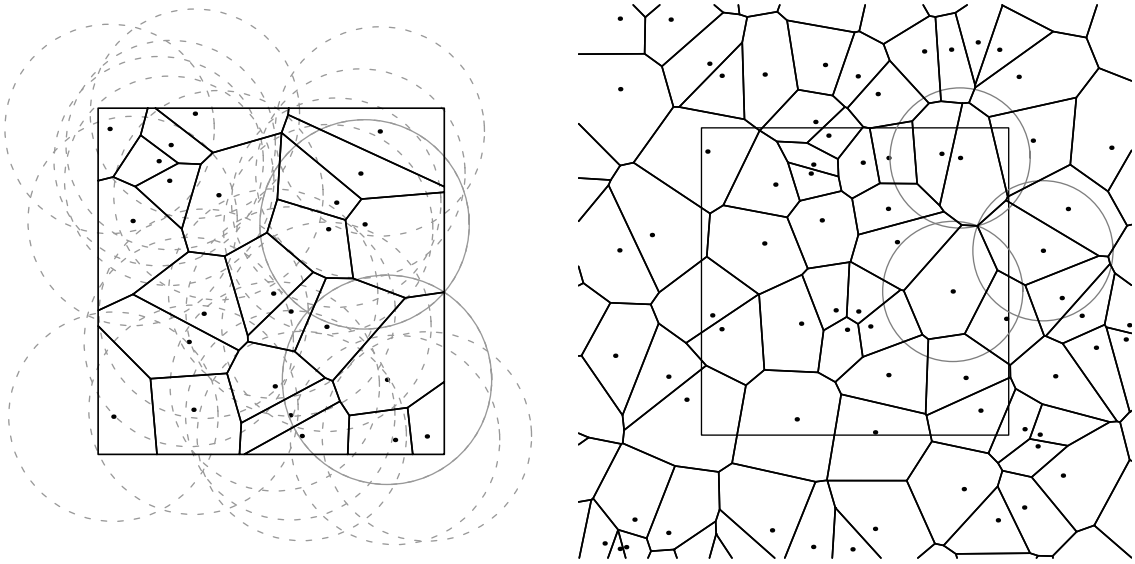

(a) (b)

Figure 2: Example of the threshold range for full coverage when a) 25 sensors are placed randomly inside the unit square, and b) on average 25 sensors per unit area are scattered uniformly over the whole plane. The critical coverage ranges are shown with solid circles.

for full coverage can be deduced to be the longest distance from a sensor to the edge of its Voronoi cell in the sensors' Voronoi diagram restricted to the domain. (When the boundary of the domain is piecewise linear, it is sufficient to concentrate on cell corners.) On the other hand, when the border effect is eliminated by allowing sensors to reside outside the domain to be covered, all the sensors whose Voronoi cells intersect with the domain must be taken into account when determining the threshold range.

The probability of full coverage is difficult to evaluate analytically when the number of sensors is finite; explicit lower and upper bounds have been derived in [6]. The remainder of this subsection is devoted to presenting asymptotic results derived by Janson in [4] and adapting these results to a form suitable for application to empirical models in the remaining subsections.

The results in [4] deal with covering a fixed "big set" K with independent identically distributed random "small sets". (The theorem is quoted in a slightly restricted form, with some notations written in full for clarity.)

Let $|A|$ denote the Lebesgue measure of A and define $r(A) = \sup_{x \in A} |x|$.

Theorem 3.1. *Suppose that K is a bounded subset of $\mathbb{R}^d$, $d \geq 1$, with $|\mathrm{Boundary}(K)| = 0$, that $\mathrm{Closure}(K) \subset \mathrm{Interior}(V)$ and that $|V| < \infty$. Suppose further that A is a random convex subset of $\mathbb{R}^d$ with $\mathrm{E}|A| > 0$ and $\mathrm{E}\, r(A)^{d+\epsilon} < \infty$ for some $\epsilon > 0$, and that m is a positive integer.*

For $a > 0$, let the small sets have the same distribution as $aA + X$, where X is $\langle$a set of random points$\rangle$ uniformly distributed on V, and let $N_{a,m}$ be the number of small sets required to cover K m times.

Let $\alpha(A)$ be a constant dependent on the shape and variation of A and let U have the extreme value distribution $\mathrm{P}(U \leq u) = \exp(-e^{-u})$. Then, as $a \to 0$,

$$\frac{\mathrm{E}|aA|}{|V|} N_{a,m} - \log \frac{|K|}{\mathrm{E}|aA|} - (d+m-1) \log\log \frac{|K|}{\mathrm{E}|aA|} + \log(m-1)! - \log \alpha \xrightarrow{d} U. \quad (3)$$

For example, $\alpha = 1$ when $d = 2$ and A is a square or a disk of fixed size, and $\alpha = 1$ always when $d = 1$ (Section 9 in [4]).

Let us now translate this theorem to the context of our sensor coverage problem. We are interested in single coverage in the plane, so $m = 1$, $d = 2$. Let K be the unit square (for reasons becoming evident shortly) and let A be the disk with unit radius representing a single sensor – hence, A is no longer random so $\mathrm{E}|aA| \equiv |aA|$, and $\alpha = 1$. For convenience of notation, we replace a with r, thus making the area $|aA| = \pi r^2$. Equation (3) now gets the form

$$\lim_{r \to 0} \mathrm{P}\left[\frac{\pi r^2}{|V|} N_r + \log \pi r^2 - 2 \log(-\log \pi r^2) \leq u \right] = \exp(-e^{-u}),$$

where we have dropped the subscript $m = 1$ from $N_{r,m}$. Instead of expressing this result in terms of the number of disks N_r needed with a given r, we may as well use the threshold range for full coverage – denote this with R_n – with a given number of disks n: either way, this result characterizes the asymptotic joint distribution of the number of sensors and their range required for full coverage. We may therefore write equivalently

$$\lim_{n \to \infty} \mathrm{P}\left[\frac{n}{|V|} \pi R_n^2 + \log \pi R_n^2 - 2 \log(-\log \pi R_n^2) \leq u \right]$$

$$= \exp(-e^{-u}), \tag{4}$$

which gives us the asymptotic distribution of the threshold range for full coverage.

The purpose of having the set V completely encompass K in Theorem 3.1 is to avoid complications resulting from the otherwise likely event that the boundary of K is the last part to be covered. In other words, the results above apply to the case without border effects as depicted in Figure 2(b). As a counterexample to the condition $\mathrm{Closure}(K) \subset \mathrm{Interior}(V)$, the author in [4] lets $V = K = [0,1]^2$ and the set $A = [-1/2, 1/2]^2$, i.e. he considers covering the unit square with small squares of side a and centers uniformly distributed inside the unit square. Under these assumptions, he derives the following:

Corollary 3.1. *Let $V = K$ be the unit square $[0,1]^2$ and let A be the square $[-1/2, 1/2]^2$. Take $m = 1$. Then*

$$\frac{\mathrm{E}|aA|}{|V|} N_{a,m} - \log \frac{|K|}{\mathrm{E}|aA|} - (d+m-1) \log\log \frac{|K|}{\mathrm{E}|aA|} + \log(m-1)! - \log\alpha \xrightarrow{d} U \tag{5}$$

with $\mathrm{P}(U \le u) = \exp(-2e^{-u/2} - e^{-u})$.

(The derivation is shown in Appendix.) The conclusion is that the asymptotic behavior is governed exclusively by the border of K, the interior being covered much sooner. The probability density functions of the distributions involved in Theorem 3.1 and Corollary 3.1 are shown in Figure 3.

Looking at the derivation of Corollary 3.1, we see that if we choose the set A to be a disk, the case becomes more complicated and the result no longer holds. Namely, with the choice of the square, the problem involving border effects could be decomposed into subproblems in one and two dimensions, both free of border effects. In the case of a disk, covering the edge of the unit square no longer implies covering the strip between the edge and the interior, and this decomposition is no longer applicable. We may however conjecture that the real distribution does not differ much from the one in Corollary 3.1. To assume the contrary, consider

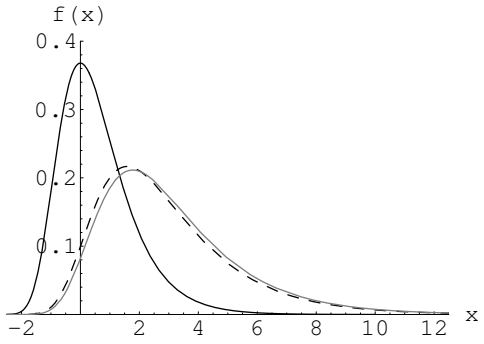

Figure 3: The probability density function involved in Theorem 3.1 (solid) and Corollary 3.1 (dashed)

the very conservative bound obtained by replacing the square with side a with a disk with radius $r = a/\sqrt{2}$ that encompasses the square. Accordingly, we may substitute $\mathrm{E}|aA| = a^2 = 2r^2 = (2/\pi) \cdot \pi r^2 = k \cdot \pi r^2$, where $k = 2/\pi$, into the result of Corollary 3.1:

$$k\pi r^2 N_r - \log(k\pi r^2)^{-1} - 2\log\log(k\pi r^2)^{-1} \xrightarrow{d} U.$$

Switching again the role of the random variable and keeping in mind the fairly centralized distribution of U (see Figure 3), we may say that in the limit, for a fixed probability of coverage, i.e. a fixed quantile in the distribution,

$$k\pi R_n^2 n \approx \log(k\pi R_n^2)^{-1} + 2\log\log(k\pi R_n^2)^{-1} \stackrel{\mathrm{def}}{=} f(n),$$

i.e. $k\pi R_n^2 n$ increases approximately like the function $f(n)$. Substituting $k\pi R_n^2$ recursively into the first logarithm yields

$$\begin{aligned} k\pi R_n^2 n &\approx \log n - \log f(n) + 2\log\log(k\pi R_n^2)^{-1} \\ &= \log n + O(\log\log n), \end{aligned} \tag{6}$$

because $2\log\log(k\pi R_n^2)^{-1}$ dominates $-\log f(n)$. This means however that $n\pi R_n^2$ – the average number of disks covering any fixed point (ignoring complications at the boundary) – increases with n like $1/k \cdot \log n$ with $1/k > 1$ which, by the observations made in e.g. [7] and [8], implies that the probability of full coverage tends to one asymptotically. Thus this conservative bound clearly overshoots the real asymptotic distribution.

On the other hand, we may repeat the steps in the derivation of Corollary 3.1 with the set A chosen as a disk with unit radius, making aA a disk with radius a. With this choice, as shown in Appendix, requiring only that the interior $[a, 1-a]^2$ of the unit square and its normal projections to the boundary are covered results in the distribution function $\mathrm{P}(U \le u) = \exp(-\frac{4}{\sqrt{\pi}} e^{-u/2} - e^{-u})$ in Corollary 3.1; this distribution is shown in gray in Figure 3. We will assume that given these coverings, the remaining parts will also be covered asymptotically with very high probability. Therefore, in what follows, we estimate the correct asymptotic distribution for the threshold range for full coverage, when the set A is a disk and $V = K$ is the unit square, with

$$\begin{aligned} &\lim_{n\to\infty} \mathrm{P}\left[n\pi R_n^2 + \log \pi R_n^2 - 2\log(-\log \pi R_n^2) \le u\right] \\ &= \exp\left(-\frac{4}{\sqrt{\pi}} e^{-u/2} - e^{-u}\right). \end{aligned} \tag{7}$$

3.2 Empirical models, a setting with border effect

Let us now focus on the case depicted in Figure 2(a) and work under the assumption presented in (7). We define

$$n\pi R_n^2 + \log \pi R_n^2 - 2\log(-\log \pi R_n^2) = \alpha(n, R_n).$$

Note that with fixed n, this is a monotonically increasing function of R_n. Hence the event $\{R_n \le r\}$ is equivalent

to $\{\alpha(n, R_n) \leq \alpha(n, r)\}$, which implies that their probabilities are also equal. Therefore, if r_q is the q-quantile of R_n (with given n), $\alpha(n, r_q)$ is that same quantile of $\alpha(n, R_n)$. Because of this one-to-one mapping between fixed quantiles of R_n and $\alpha(n, R_n)$, each can be solved given the other, either by direct substitution (when r_q is known) or numerically (in the other direction). Thus, if we have a model that gives us a desired quantile of $\alpha(n, R_n)$ with given n, we can find the same quantile of R_n, i.e., the value of the sensing range that, with n randomly placed sensors, provides full coverage with the probability corresponding to the quantile.

With this in mind, fixing the right hand side of (7) to a certain probability q (corresponding to $u_q = -2\log(\sqrt{4/\pi - \log q} - 2/\sqrt{\pi})$) shows that as n tends to infinity, the q-quantile of $\alpha(n, R_n)$ – denote this by $\alpha_q(n)$ – tends to the constant u_q. This allows us to find empirical models for individual quantiles of $\alpha(n, R_n)$ when n is finite, with the correct limit u_q in the asymptotic distribution, by using quantile estimates of R_n obtained by simulation. As shown above, these models in turn serve as quantile models for R_n: one only needs to solve r_q numerically from the model of $\alpha_q(n)$ with the value of n of interest. (Or, alternatively, to solve n given the range: the model can be thought of as a curve in the n/r-plane representing the constant probability q.)

The statistical behavior of R_n in the unit square was simulated with n varying in the range from 10 to 350 and using a sample size of 5000. As an example, Figure 4 demonstrates the quantitative difference between expected area coverage and the probability of full coverage. Even though the two curves are not directly comparable, the figure shows that for any significant probability of full coverage, the expected area coverage must be very high.

In Figure 5(a) the estimates of $\alpha_{0.5}(n)$ – obtained by substituting the estimated medians of R_n into $\alpha(n, R_n)$ – are given, together with a fitted regression model of the

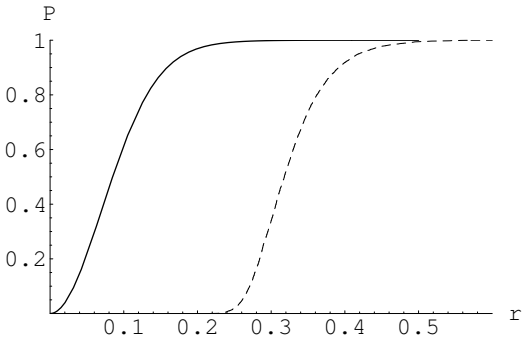

Figure 4: The expected area coverage in a circular domain according to (1) (solid line) and the empirical cumulative distribution of the threshold range for full coverage in a square domain (dashed line) when $n = 100$. In both cases, the unit of the range has been chosen so that the area of a coverage disk with radius 1 is equal to that of the domain.

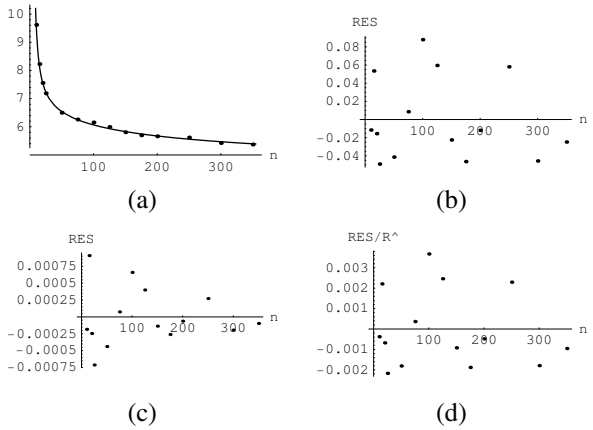

Figure 5: The model (a) and its residuals (b) obtained for $\alpha_{0.5}(n)$, and the overall absolute (c) and relative (d) residuals for the 50% quantile of R_n.

form

$$\alpha_q(n) = an^{-b} + cn^{-d} + u_q, \qquad a, b, c, d > 0, \quad (8)$$

i.e. a composite power law where a slow-decaying component characterizes the tail of the model and the more rapid supplement describes the behavior up to $n \approx 50$. Figures 5(b-d) show the residuals (the differences between the data points and the fitted model) plotted for the model for $\alpha_{0.5}(n)$ and the corresponding model for the median of R_n. We see that the residuals do not show any visible trend, meaning that the overall statistical trend is well captured by the model. It is also worth noting that Figures 5(b) and 5(d) are almost identical in pattern, which implies that fitting the parameters by minimizing the sum of squared errors of $\alpha_q(n)$ is nearly equivalent to minimizing the sum of squared relative residuals of the q-quantile of R_n. This is a sensible choice because, as shown by Figure 5(c), the variance of R_n (and hence that of its quantile estimates) decreases with n, and the data points with smaller variance yield more accurate information and therefore deserve more emphasis when fitting the model.

The 50% quantile was chosen for building the model to maximize the accuracy of the quantile estimates obtained from limited-size samples. However, the model (8) is applicable to other quantiles as well: Figure 6 depicts the relative residuals for other selected quantile models for R_n. The parameter estimates for all these models are given in Table 1. Parameter a shows a steady increase with the quantile, whereas the magnitude of parameter b does not seem to change significantly. The estimates for the parameters c and d develop in an inconsistent manner from one quantile to the next and therefore convey little useful information. This behavior is due to the fact that as the quantile increases, fewer data points within $n < 50$ satisfy the condition $|K|/(\pi R_n^2) > 1$ required for $\alpha(n, R_n)$ to be real-valued and can be used in estimating the parameters.

To gain some idea on the validity of these models – and also of the approximate distribution (7) – additional

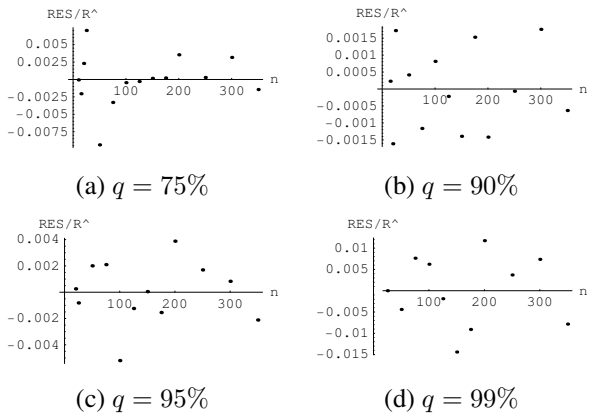

(a) $q = 75\%$ (b) $q = 90\%$

(c) $q = 95\%$ (d) $q = 99\%$

Figure 6: Relative residuals for various quantiles of R_n

Quantile	a	b	c	d
50%	7.49	0.168	253	2.11
75%	11.6	0.200	322000	4.67
90%	11.9	0.150	2120	2.42
95%	15.2	0.160	12300	2.98
99%	20.5	0.151	$3.85 \cdot 10^{31}$	22.5

Table 1: Parameter estimates for the model (8) for $\alpha_q(n)$, for different quantiles of R_n

simulations of R_n were carried out when $n = 1000$. Because of the extensive simulation times, the sample size was only 1000. Figure 7 illustrates how the predictions of the quantile models presented above relate to the empirical cumulative distribution of R_{1000}. Slight deviations are noticeable, which may be due to errors in the approximation (7) or the model (8), inaccuracy in the model parameters, or the small sample size of the validation data. The fact that the deviations do not all have the same sign makes the latter two seem more likely.

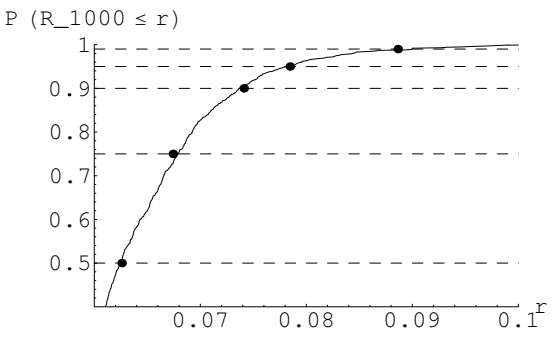

Figure 7: Predictions of five quantile models for R_{1000} and the empirical cumulative distribution

3.3 Empirical models, a setting without border effect

The case depicted in Figure 2(b) may be approached as above, by using similar models. Now we have even the exact result (4). Correspondingly, we define

$$\frac{n}{|V|}\pi R_n^2 + \log \pi R_n^2 - 2\log(-\log \pi R_n^2) = \alpha\left(\frac{n}{|V|}, R_n\right),$$

where we now include $|V|$ explicitly. Namely, we maintain the average node density $n/|V|$ at the same values as in the previous simulations for comparability. The set V where each density is applied is obtained by enlarging the unit square in all directions by a length which must be more than the threshold range for full coverage in any resulting realization (this is assured afterwards; if the requirement is not met, the set V is enlarged more and the simulations are repeated). This way, sensors outside V would not have any effect.

Figure 8 shows the behavior of the estimated medians of the threshold range for full coverage with and without border effects. For comparison, the corresponding values for the threshold range for connectivity (i.e. the longest edge length in the Euclidean minimum spanning tree of the nodes) have also been added. This shows that with low n, the latter is between the former two in magnitude. However, we may say that just as for full coverage with border effects, $n\pi r^2$ must grow like $\log n + O(\log \log n)$ also without border effects, by starting from (4) and repeating the steps leading to (6). On the other hand, we know that for connectivity, $n\pi r^2 \approx \log n$ asymptotically, as shown in [3]. This means that the two upper trails in Figure 8 must eventually cross.

Based on (4), we know now that the limit of the q-quantile $\alpha_q(n/|V|)$ of $\alpha(n/|V|, R_n)$ is $u_q = -\log \log q^{-1}$. The results of applying the model (8) again are shown in Figure 9 and Table 2. Because the threshold ranges are now smaller, data points as low as $n = 5$ could be utilized in building the models. As a

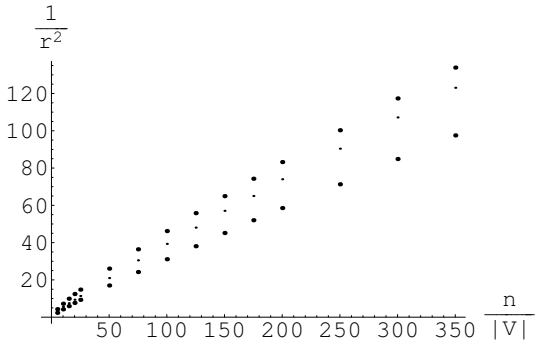

Figure 8: Squared inverses of the estimated medians of the threshold range for full coverage, without border effect (upper points), with border effect (lower points), and of the threshold range for connectivity (smaller points). All the simulations have been carried out in the unit square.

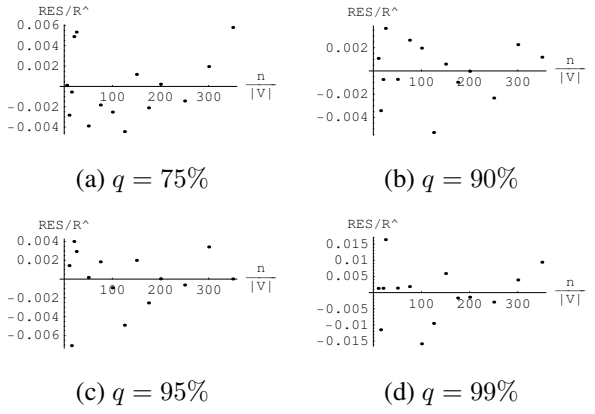

(a) $q = 75\%$ (b) $q = 90\%$

(c) $q = 95\%$ (d) $q = 99\%$

Figure 9: Relative residuals for various quantiles of R_n in the absence of border effect

Quantile	a	b	c	d
50%	3.35	0.148	17.6	1.18
75%	5.34	0.200	115	2.04
90%	3.45	0.0988	26.7	1.02
95%	4.43	0.123	57.7	1.30
99%	7.64	0.197	511	2.14

Table 2: Parameter estimates for the model (8) for $\alpha(q, n/|V|)$, for different quantiles of R_n

result – if we disregard the 75% quantile – the parameter estimates now seem to behave in a more consistent manner.

Because the uncertainty about the correct asymptotic distribution can now be ruled out, one should be entitled to assume that these models have at least as good a predictive power as those in the case of border effects.

4 Conclusions

This study focused on the area coverage of a random sensor network in a bounded domain, more specifically, the expected area coverage and the probability of full coverage. The former quantity can be addressed analytically, whereas the latter poses a difficult problem in the non-asymptotic regime. It should be pointed out at this point that also the probability of zero-coverage is trivial to solve analytically: it is the probability that no sensor exists within the common sensing range from the domain to be covered. Although not very interesting from a practical point of view, this is the only quantile of the distribution of the area coverage for which we have an analytical expression.

Regarding the problem of full coverage, the analytical results in [4] and their implications played a key role in the approach taken. By using the notion of the threshold range for full coverage and interpreting the analytical results as the asymptotic distribution of this threshold range, full coverage can be predicted using regression models describing the convergence of individual quantiles to this asymptotic distribution. In the presence of border effects, the asymptotic distribution had to be approximated. Despite this approximation, the corresponding regression models proved to have satisfactory predictive power.

The border effect is a dominant phenomenon affecting area coverage. From the viewpoint of practical applications, border effects can be ignored in sensor network design provided that the deployment region of the sensors is properly expanded. As this should be possible in most cases, the corresponding models seem more likely to have practical value.

Acknowledgements

I thank S. Janson for his enlightening clarifications regarding [4], Jorma Virtamo for helpful discussions on the matter, and the anonymous reviewers for their constructive comments. This work has been financially supported by the Academy of Finland (grant n:o 202204) and the Finnish Defence Forces Technical Research Centre, and in part by a grant from the Nokia Foundation.

Appendix

In order to account for the border effects, we need the following result from [4] (the notations of Theorem 3.1 apply):

Lemma 4.1. *Suppose that K is a bounded set in $\mathbb{R}^d$ such that $|\mathrm{Boundary}(K)| = 0$ and that $\mathrm{E}\, r(A)^{d+\epsilon} < \infty$ for some $\epsilon > 0$. Under certain conditions that hold almost surely (see Lemma 7.3 in [4]), if $a \to 0$ and*

$$\mathrm{E}|aA|\lambda(a) - \log\frac{|K|}{\mathrm{E}|aA|} - d\log\log\frac{|K|}{\mathrm{E}|aA|} - \log\alpha \to u, \quad -\infty < u < \infty, \tag{9}$$

then

$$P(\Xi_{\lambda(a),a} \text{ covers } K) \to \exp(-e^{-u}). \tag{10}$$

Here, $\Xi^V_{\lambda(a),a}$ denotes the set $\{aA_i + X_i\}$ in which X_i are the points of a d-dimensional Poisson process restricted to the set V, with intensity $\lambda(a)$. The superscript is omitted when $V = \mathbb{R}^d$. The intensity $\lambda(a)$ is defined so that the limit u holds (see Section 3 in [4]).

Now let $V = K = [0,1]^2$ and $A = [-1/2, 1/2]^2$ (hence, $\alpha = 1$). Applying Lemma 4.1, supposing that $a \to 0$ and $a^2\lambda(a) - \log a^{-2} - 2\log\log a^{-2} \to u$, implies that $\mathrm{P}(\Xi^V_{\lambda(a),a}$ covers $[a/2, 1-a/2]^2) \to \exp(-e^{-u})$ since $\Xi^V_{\lambda(a),a}$ and $\Xi_{\lambda(a),a}$ coincide on this interior of $[0,1]^2$. However, on the boundary, e.g., on $\{0\} \times [a/2, 1-a/2]$, $\Xi^V_{\lambda(a),a}$ consists of intervals of length a with intensity $\lambda_1(a) = a\lambda(a)/2$. Since by the earlier limit u, $a\lambda_1(a) - \log a^{-1} - \log\log a^{-1} \to$

$u/2 + \log 2$, Lemma 4.1 yields P($\Xi^V_{\lambda(a),a}$ covers $\{0\} \times [a/2, 1-a/2]) \to \exp(-\frac{1}{2}e^{-u/2})$. Covering the (interior of the) edge $\{0\} \times [a/2, 1-a/2]$ in turn implies covering the strip $[0, a/2] \times [a/2, 1-a/2]$ between the edge and the interior $[a/2, 1-a/2]^2$. Although not independent events, the probability of covering K is asymptotically obtained as the product of probabilities of covering the interior and its normal projections to the boundaries: P($\Xi^V_{\lambda(a),a}$ covers K) $\to \exp(-2e^{-u/2} - e^{-u})$. This is equivalent to Corollary 3.1.

Then let A be a disk with unit radius (recall that thus again $\alpha = 1$). Now, letting $a \to 0$ and $\pi a^2\lambda(a) - \log(\pi a^2)^{-1} - 2\log\log(\pi a^2)^{-1} \to u$, we have P($\Xi^V_{\lambda(a),a}$ covers $[a, 1-a]^2) \to \exp(-e^{-u})$ by Lemma 4.1. On the boundary $\{0\} \times [a, 1-a]$, $\Xi^V_{\lambda(a),a}$ has intensity $\lambda_1(a) = a\lambda(a)$ and consists of intervals of length $2\sqrt{a^2 - D^2}$ where the distance D of the disk center from the boundary is uniformly distributed in $[0, a]$; the expected length is $\pi a/2$. In order to utilize Lemma 4.1, we now wish to evaluate the limit of $\pi a^2\lambda(a)/2 - \log(\pi a/2)^{-1} - \log\log(\pi a/2)^{-1}$ with respect to u. To do this, we write $\pi a^2 = (\pi a/2)^2(2/\sqrt{\pi})^2$ and develop the limit u as follows:

$$
\begin{aligned}
u \leftarrow & \pi a^2\lambda(a) - \log(\pi a^2)^{-1} - 2\log\log(\pi a^2)^{-1} \\
= & 2\left(\frac{\pi a^2\lambda(a)}{2} - \log(\pi a/2)^{-1} - \log\frac{\sqrt{\pi}}{2}\right. \\
& \left. - \log\left(2\log(\pi a/2)^{-1} - 2\log\frac{2}{\sqrt{\pi}}\right)\right) \\
= & 2\left(\frac{\pi a^2\lambda(a)}{2} - \log(\pi a/2)^{-1} - \log\frac{\sqrt{\pi}}{2}\right. \\
& \left. - \log 2 - \log\left(\log(\pi a/2)^{-1} - \log\frac{2}{\sqrt{\pi}}\right)\right) \\
\Leftrightarrow & \\
& \pi a^2\lambda(a)/2 - \log(\pi a/2)^{-1} - \log\log(\pi a/2)^{-1} \\
\to & \frac{\pi a^2\lambda(a)}{2} - \log(\pi a/2)^{-1} - \log\left(\log(\pi a/2)^{-1}\right. \\
& \left. - \log\sqrt{4/\pi}\right) \\
\to & u/2 + \log\sqrt{\pi}
\end{aligned}
$$

as $a \to 0$, since in this limit $\log\left(\log(\pi a/2)^{-1} - \log\sqrt{4/\pi}\right) - \log\log(\pi a/2)^{-1} \to 0$. Lemma 4.1 now yields P($\Xi^V_{\lambda(a),a}$ covers $\{0\} \times [a, 1-a]) \to \exp(-\frac{1}{\sqrt{\pi}}e^{-u/2})$. Accordingly, the probability that the interior $[a, 1-a]^2$ and its normal projections to the boundary are covered with the specified intensity has the limit $\exp(-\frac{4}{\sqrt{\pi}}e^{-u/2} - e^{-u})$.

References

[1] B. Liu and D. Towsley, "On the coverage and detectability of large-scale wireless sensor networks," in *Proceedings of the Workshop on Modeling and Optimization in Mobile, Ad Hoc and Wireless Networks (WiOpt'03)*, Mar. 2003.

[2] M. Sánchez, P. Manzoni, and Z. J. Haas, "Determination of critical transmission range in Ad-Hoc Networks," in *Proceedings of Multiaccess Mobility and Teletraffic for Wireless Communications 1999 Workshop (MMT'99)*, Oct. 1999.

[3] M. D. Penrose, "The longest edge of the random minimal spanning tree," *Annals of Applied Probability*, vol. 7, no. 2, 1997.

[4] S. Janson, "Random coverings in several dimensions," *Acta Mathematica*, vol. 156, 1986.

[5] E. Weisstein, "Circle-Circle Intersection," *From* MathWorld – *A Wolfram Web Resource*, June 2004. [Online]. Available: http://mathworld.wolfram.com/Circle-CircleIntersection.html

[6] P. Hall, *Introduction to the theory of coverage processes*. John Wiley & Sons, 1988.

[7] T. K. Philips, S. S. Panwar, and A. N. Tantawi, "Connectivity properties of a packet radio network model," *IEEE Transactions on Information Theory*, vol. 35, no. 5, Sept. 1989.

[8] P. Gupta and P. R. Kumar, "Critical power for asymptotic connectivity in wireless networks," *Stochastic Analysis, Control, Optimization and Applications: A Volume in Honor of W.H. Fleming*, 1998.